


# Lifetimes and energetics of the first electronically excited states of NaH<sub>2</sub>O from time-resolved photoelectron imaging

**Journal Article****Author(s):**

Gartmann, Thomas E.; Yoder, Bruce L.; Chasovskikh, Egor; [Signorell, Ruth](#) 

**Publication date:**

2017-09-01

**Permanent link:**

<https://doi.org/10.3929/ethz-b-000128621>

**Rights / license:**

[Creative Commons Attribution-NonCommercial-NoDerivatives 4.0 International](#)

**Originally published in:**

Chemical Physics Letters 683, <https://doi.org/10.1016/j.cplett.2017.01.044>

# Lifetimes and energetics of the first electronically excited states of NaH<sub>2</sub>O from time-resolved photoelectron imaging

Thomas Gartmann, Bruce L. Yoder, Egor Chasovskikh, and Ruth Signorell<sup>1,\*</sup>

Department of Chemistry and Applied Biosciences, Laboratory of Physical Chemistry, ETH Zürich, Vladimir-Prelog-Weg 2. CH-8093 Zürich, Switzerland

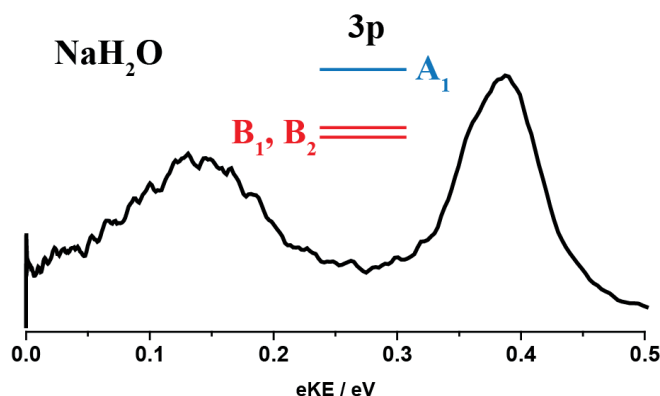
\*Correspondence to: rsignorell@ethz.ch.

## ABSTRACT

The energetics and lifetimes of the first electronically excited states (“3p-states”) of NaH<sub>2</sub>O and NaD<sub>2</sub>O have been measured by pump-probe (740/780 and 400 nm) photoelectron imaging. The photoelectron spectra of NaH<sub>2</sub>O show two bands at an electron kinetic energy of 0.14 and 0.38 eV, respectively. We assign the former to excitation via the two energetically close lying “p<sub>π</sub>-states” with flat potential curves in the intermolecular degrees of freedom, and the latter to the excitation via the “p<sub>σ</sub>-state” characterized by significantly steeper potential curves. The relaxation of all “p-states” follows a double exponential decay with a lifetime around 110 ps for the dominant fast component.

**Keywords:** time-resolved photoelectron spectroscopy, angle-resolved photoelectron spectroscopy, pump-probe femtosecond spectroscopy, photoelectron anisotropy, molecular clusters, excited state dynamics, quantum beats

## TOC graphic



## 1. Introduction

The interest sodium-doped water clusters ( $\text{Na}(\text{H}_2\text{O})_n$ ) [1-15] and anion water clusters ( $(\text{H}_2\text{O})_n^-$ ) [16-22] have attracted is attributed to their role as prototype systems for clarifying the mechanism of the emergence of the hydrated electron [23,24]. The dynamics of electronically excited states of the hydrated electron has received special attention in the context of electron initiated chemical processes and radiation damage of biological matter [7,9-11,19,25-29]. Schulz and coworkers have studied the lifetimes of  $\text{Na}(\text{H}_2\text{O})_n$  for  $n = 2-40$  after excitation from the ground state to the lowest lying electronically excited “p-states” (“s  $\rightarrow$  p” transition) with pump-probe ion and electron spectroscopy [10,11]. For simplicity we use here the nomenclature of the corresponding states and transitions in the Na atom. The observed, rapid decrease of the excited-state lifetime from 1.3 ps for  $n = 2$  to  $\sim 100$  fs for  $n \geq 10$  was attributed to a combination of solvent rearrangement and internal energy conversion. Using ion depletion spectroscopy in combination with theoretical studies by Hashimoto and coworkers, they investigated the energetics of the lowest manifold of p-states as a function of solvent cluster size [7,9]. For  $n \geq 2$ , very broad absorption bands were found, consistent with interior cluster structures where the Na atom is surrounded by water clusters. The s  $\rightarrow$  p absorption band of  $\text{NaH}_2\text{O}$  could not be fully observed because of a gap in the laser energy between 1.69 and 1.80 eV. However, an onset value of  $\sim 1.67$  eV and a width of  $\sim 0.15$  eV were determined [7,8].

In this work, we focus on  $\text{NaH}_2\text{O}$  and investigate the dynamics and energetics of its lowest lying p-states with time-resolved photoelectron imaging. This weakly-bound complex is of particular interest as a benchmark system for theoretical studies as it is small enough that even a full-dimensional treatment is conceivable [30]. The first three excited p-states lie energetically very close and are well separated from higher electronic states (Fig. 1, [7,9]) – a situation that results in interesting vibronic couplings. For the  $\text{NaH}_2\text{O}$  ground state, the calculations by Hashimoto and coworkers predict a pyramidal ( $C_s$ ) equilibrium structure [8,9]. In Fig. 1, we show the energy-dependence of the ground state, the first three electronically excited p-states, and the ground state of the ion as a function of the out-of-plane angle  $\delta$  (panel a) and the Na-O distance (panel b). We label the various curves with the electronic symmetry to which they correlate in the  $C_{2v}$  configuration. The ground state energy (full black line; X) is calculated with MP2/aug-cc-pVTZ. We find a similar ground state  $C_s$  structure as Hashimoto at an out-of-plane angle around  $\delta = 20^\circ$ . However, the potential as a function of  $\delta$  is extremely flat, which is confirmed by higher-level CCSD(T)/aug-cc-pCVQZ

calculations (not shown). The black dotted-dashed line indicates the corresponding ground state wavefunction  $\Psi_\delta$ , which is that of quasi-planar, very floppy complex, extending to very large  $\delta$  angles. The method used for the vibrational calculation is described in refs. [31,32].

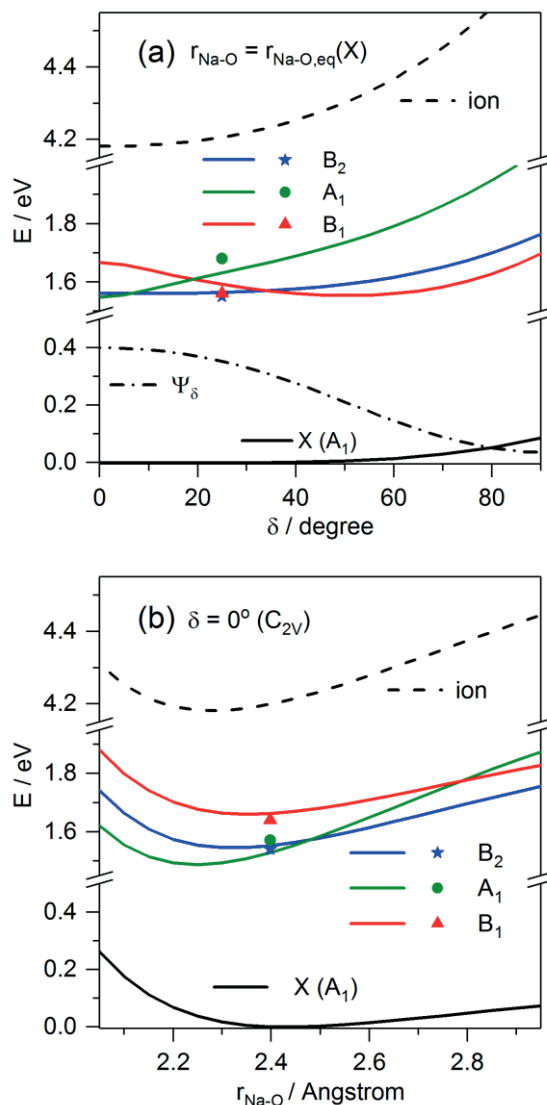


**Figure 1:** Calculated energies of the ground state (full black line), the first three electronically excited states (full blue, green, and red line), and the ionic state (dashed black line) of  $\text{NaH}_2\text{O}$  as a function of the out-of-plane angle  $\delta$  (panel a) and the Na-O distance (panel b).  $\delta$  is the angle between the bisector of the  $\text{H}_2\text{O}$  unit and the Na-O “bond”.  $\delta = 0^\circ$  corresponds to the  $C_{2v}$  structure  $\text{Na}\cdots\text{OH}_2$ . The dashed-dotted black line shows the ground state wavefunction  $\Psi_\delta$ . See text for calculation methods. The symbols (blue stars, green circles, and red triangles) represent the calculations of the electronically excited states by Hashimoto and coworkers [7,9].

For the first electronically excited p-states, Hashimoto and coworkers calculated three close-lying states within roughly 0.13 eV, two of which are virtually degenerate ( $< 0.03$  eV) [7,9]. Hashimoto's data for the respective geometry ( $C_s$  and  $C_{2v}$ , respectively) are indicated as symbols in Fig. 1. The most striking aspect is the interchange of the order depending on the symmetry of the structure. We have studied the qualitative geometry-dependence of the excited states energies more closely by calculating the excitation energies at the various MP2 ground state energies. The excitation energies were calculated at the CIS(D) level following ref. [33], which includes 2<sup>nd</sup> order corrections to the CIS energies. Fig. 1 reveals a complicated arrangement of crossing electronically excited levels. The multiple crossings of near degenerate excited electronic states combined with the low vibrational frequencies of this floppy system [7,9], will lead to extensive vibronic coupling. The dashed, black curve, which represents the ionic ground state ( $\text{NaH}_2\text{O}^+$ ) shows the typical behaviour of a semi-rigid molecule [34]; i. e. a relatively steep potential curve with a single well-defined quasi-harmonic minimum. The corresponding wavefunction (not shown) is confined to the vicinity of the planar  $C_{2v}$  structure. The experimental adiabatic ionization energy (AIE) of  $\text{NaH}_2\text{O}$  of 4.38 eV [35] corresponds to a shift of -0.76 eV relative to the ionization energy (IE) of bare Na atoms [36]. This compares well with our calculated value of -0.73 eV. The general situation depicted in Fig. 1 lets us expect a pronounced energy-dependence of the overall Franck-Condon factor for the pump and probe steps.

## 2. Experimental section

We report here the first measurements with a new experimental setup, which consists of a supersonic expansion and a Na-pickup chamber for cluster formation, a 1kHz femtosecond laser system, and a velocity map photoelectron spectrometer [37,38]. Details of the new setup will be provided in a forthcoming publication. A continuous supersonic beam of  $\text{H}_2\text{O}$  and He traverses a Na-pickup chamber with a Na-oven [39,40] where  $\text{NaH}_2\text{O}$  complexes are formed. Note that a certain fraction of larger  $\text{Na}(\text{H}_2\text{O})_n$  ( $n \geq 2$ ) clusters are also formed. The lifetimes of the excited p-states of these larger clusters are much shorter than those of the  $\text{NaH}_2\text{O}$  p-states (see below Figs. 2 and 3). For this reason, the signatures of the larger clusters in the photoelectron spectra can be clearly distinguished from those of  $\text{NaH}_2\text{O}$ .  $\text{NaH}_2\text{O}$  complexes are excited to the p-states with a fs pump pulse of  $\lambda_{\text{pump}} = 780$  nm or 740 nm. The excited  $\text{NaH}_2\text{O}$  complexes are then ionized with a time-delayed probe pulse of  $\lambda_{\text{probe}} = 400$  nm.

Pump and probe pulses are linearly polarized parallel to the detector plane and their cross-correlation is less than 100 fs. Velocity-map images (VMI) are recorded with a similar spectrometer as described in refs. [37,38,41], but at a 1kHz rate using a CMOS camera and subsequent centroiding. The time-dependent raw photoelectron images were reconstructed with the MEVIR program [42]. The photoelectron angular distributions (PADs) are described by an expansion of Legendre polynomials  $P_{2i}$  with anisotropy parameters  $\beta_{2i}$ , defined by [43].

$$I(E, \theta, \Delta t) \propto \frac{\sigma(E, \Delta t)}{4\pi} \sum_{i=0}^2 \beta_{2i}(E, \Delta t) P_{2i}(\cos \theta) \quad \text{Eq. (1)}$$

Where  $E$  is the photoelectron kinetic energy,  $\theta$  is the angle between the polarization vector and the ejection direction of the photoelectrons,  $\Delta t$  is the pump-probe time-delay,  $I$  is the angular intensity distribution of the photoelectrons, and  $\sigma$  is the total photoionization cross section. The time-dependent, relative abundance of the different species in the molecular beam ( $\text{NaH}_2\text{O}$ ,  $\text{Na}(\text{H}_2\text{O})_n$  with  $n \geq 2$ ,  $\text{Na}$ , and  $\text{Na}_2$ ) was monitored with time-of-flight mass spectrometry after two-photon ionization by the pump and probe (Fig.3). To determine the influence of deuteration, we have also recorded data for  $\text{NaD}_2\text{O}$ .

### 3. Results and discussion

#### 3.1 Time-resolved photoelectron spectra

Fig. 2a shows a colour map of the time-resolved photoelectron spectra (TRPES) recorded at a pump wavelength of 740 nm. Selected photoelectron spectra (PES) at five different pump probe delays  $\Delta t$  between -0.4 and +100.7 ps are depicted in Fig. 2b. Four distinct photoelectron bands are visible at electron kinetic energies (eKEs) of 0.14, 0.38, ~0.7, and 1.06 eV with varying contributions as a function of time. These bands are referred to as  $p_1$ ,  $p_2$ ,  $p_3$ , and  $p_4$ . The band  $p_4$  is already present when the probe laser arrives before the pump laser ( $\Delta t \leq 0$  ps) and does not vary as a function of  $\Delta t$  for  $\Delta t \lesssim 1000$  ps. We assign this band to the two-photon ionization of bare Na atoms by the probe laser (400 nm), in agreement with the observed eKE of 1.06 eV for an ionization energy (IE) of Na of 5.14 eV [36] and with the time-independence of the total  $\text{Na}^+$  ion signal from the time-resolved mass spectra (Fig. 3). Fig. 3 also includes a constant contribution of  $\text{Na}_2^+$  ions. Excitation and ionization of  $\text{Na}_2$  by the pump and probe laser, respectively, lead to a hardly visible, constant electron signal at

$\sim 0.02$  eV (asterisks in Figs. 2b and d), which is consistent with the available total photon energy and the IE of  $\text{Na}_2$  [44]. Both the Na and the  $\text{Na}_2$  background arises from the effusive Na-beam that is formed at the aperture between the Na-pickup chamber and the ionization chamber.

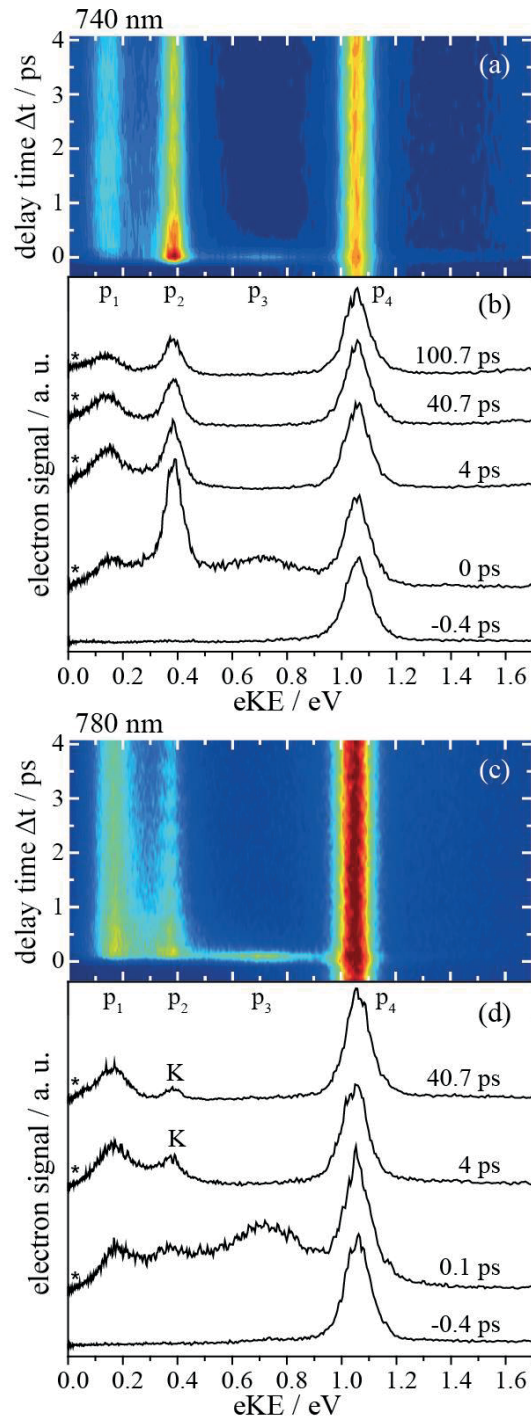


**Figure 2:** Time-resolved photoelectron spectra of  $\text{NaH}_2\text{O}$  ( $p_1$  and  $p_2$ ),  $\text{Na}(\text{H}_2\text{O})_n$  with  $n \geq 2$  ( $p_1$ ,  $p_2$ , and  $p_3$ ) and Na ( $p_4$ ) as a function of the electron kinetic energy (eKE) and the pump-

probe delay  $\Delta t$ . a) and b) TRPES recorded at a pump wavelength of 740 nm. c) and d) TRPES recorded at a pump wavelength of 780 nm. The beat signal at 0.38 eV in panel c arises from the coherent excitation of the two 4p spin-orbit components of K atom impurities. The asterisks in panels b and d label the very small electron signals from  $\text{Na}_2$ .

The electron signals of the remaining three bands  $p_1$ - $p_3$  are time-dependent. At early times ( $\approx 2$ ps), the bands are only partly resolved and the signals decrease continuously with increasing time. The signals  $p_1$  and  $p_2$  become stable after about 3-4 ps, while  $p_3$  disappears completely. The energetics and the temporal evolution of  $p_1$ ,  $p_2$  and  $p_3$  at early times is fully consistent with an assignment of these bands to the ionization after p-state excitations of small  $\text{Na}(\text{H}_2\text{O})_n$  clusters with  $2 \leq n \leq 8$ . Clusters with  $n \geq 2$  show photoelectron signals in the whole region below  $\sim 1$  eV eKE, which disappear after a few ps because of the short excited state lifetimes of these clusters [10,11]. The fast disappearance of the cluster electron signals for  $n \geq 2$  is also consistent with the temporal evolution of the corresponding cluster ion signals shown in Fig. 3. Fig. 3 also shows that  $\text{NaH}_2\text{O}^+$  is the only long-lived cluster. Therefore, the electron signals  $p_1$  and  $p_2$  that remain visible in Figs. 2a and b beyond  $\sim 3$ -4 ps must both arise from the  $\text{NaH}_2\text{O}$  complex. This assignment is supported by the lifetimes of the electron signals  $p_1$  and  $p_2$  and the  $\text{NaH}_2\text{O}^+$  ion signal (Figs. 3 and 4). Upon deuteration, only the  $p_1$  band shifts significantly to higher energy by a few 0.01 eV, while the  $p_2$  band in  $\text{NaD}_2\text{O}$  remains unshifted within our uncertainty. As will be discussed in section 3.3, the observation of two distinct electron signals for  $\text{NaH}_2\text{O}$  qualitatively agrees with the energetics of the p-states in Fig. 1.

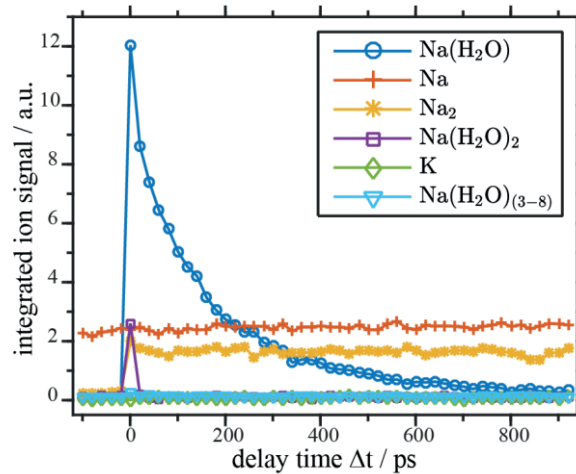


**Figure 3:** Time-dependent cluster ion signals of  $\text{NaH}_2\text{O}^+$ ,  $\text{Na}^+$ ,  $\text{Na}_2^+$ ,  $\text{Na}(\text{H}_2\text{O})_2^+$ ,  $\text{K}^+$ , and  $\text{Na}(\text{H}_2\text{O})_n^+$  with  $n > 2$  obtained from mass spectra recorded as a function of the pump-probe



delay  $\Delta t$  with a pump wavelength of 740 nm. Note that the  $K^+$ , and  $Na(H_2O)_{n=3-8}^+$  are difficult to distinguish because they lie on top of each other. The lines serve as a guide to the eye.

While we observe two bands for  $NaH_2O$  at a pump energy of 1.68 eV (740 nm) and a total photon energy of 1.68 eV + 3.10 eV = 4.78 eV, Schulz and coworkers only observed the  $p_1$  band at a lower total photon energy of 1.56 eV + 3.12 eV = 4.68 eV [11]. In both cases, the total available photon energy exceeds the AIE of  $NaH_2O$  (4.38 eV [35]) by about  $\sim 0.3$  eV. We have performed additional measurements at a pump energy of 1.59 eV (780 nm), which yield a total photon energy (4.69 eV) almost identical to that used by Schulz and coworkers [11]. The  $p_2$  band in Figs. 2c and d at a pump wavelength of 780 nm is indeed much weaker than at a pump wavelength of 740 nm (Figs. 2a and b). At short times it is dominated by contributions from  $Na(H_2O)_n$  with  $n \geq 2$  as described above. However, even at longer times ( $> 3-4$  ps) when the excited states of all larger clusters have already decayed, the  $p_2$  signal in Figs. 2 c and d does not disappear - in contrast to the observation by Schulz and coworkers. Most remarkably, it shows a beat structure with a period of  $584 \pm 8$  fs persisting over more than 700 ps. We also observed an identical beat structure in the corresponding anisotropy parameters  $\beta_2$  and  $\beta_4$  (not shown). Quantum beat spectroscopy; i. e. the time-dependent observation of a system following coherent excitation of eigenstates; has been applied to various atomic and molecular systems using laser excitation ranging from the nanosecond to the attosecond regime [45-48]. However, the observation of quantum beat signals after coherent femtosecond excitation of the p-states of  $NaH_2O$  appears very unlikely given the complex rovibronic structure (Fig. 1). Moreover, the  $p_2$  electron signal remains constant over the decay lifetimes of  $NaH_2O$  (section 3.2), so that it cannot arise from this species. An evaluation of the energetics and the beat signature shows that it cannot arise from Na or  $Na_2$  either, thus hinting at another source with a long lifetime. A careful inspection of the mass spectrum indeed revealed a tiny impurity of potassium (K). Small amounts of K ( $< 0.03\%$ ) are present in the Na sample and thus in the effusive beam. A beat period of  $584 \pm 8$  fs corresponds to an energy difference of  $57.1 \text{ cm}^{-1}$ , which perfectly agrees with the fine structure splitting of the  $^2P_{1/2}$  and  $^2P_{3/2}$  levels of K at 12985.186 and 13042.896  $\text{cm}^{-1}$ , respectively [49]. The observed eKE of 0.38 eV of the beating signal is also consistent with the IE of K [49] within the laser bandwidths. Our results at a pump wavelength of 780 nm are thus in agreement with the results of Schulz, namely that for  $NaH_2O$  only the electron signal  $p_1$  is observed at this lower pump energy.

### 3.2 Excited state lifetimes and anisotropy parameters

We have determined the excited state lifetimes of the  $p_1$  and  $p_2$  electron signal of  $\text{NaH}_2\text{O}$  (Fig. 4 a and b, respectively) and of the  $\text{NaH}_2\text{O}^+$  ion signal (trace c). Similar to ref. [10], we used a bi-exponential function with a short and a long relaxation time  $\tau_1$  and  $\tau_2$ , respectively, to describe the decay of the electron signal:

$$I(\Delta t) = C + A_1 \cdot \exp\left(-\frac{\Delta t}{\tau_1}\right) + A_2 \cdot \exp\left(-\frac{\Delta t}{\tau_2}\right) \text{ Eq. (2)}$$

$I$  is the electron signal,  $\Delta t$  is the pump-probe delay, and  $C$ ,  $A_1$  and  $A_2$  are fitting constants. At a pump energy of 740 nm, we obtain  $\tau_1 = 100 \pm 20$  ps and  $\tau_2 = 390 \pm 320$  ps for the electron signal  $p_1$  and  $\tau_1 = 120 \pm 50$  ps and  $\tau_2 = 390 \pm 350$  ps for the electron signal  $p_2$ . The fast excited state lifetime  $\tau_1$  of  $\text{NaH}_2\text{O}$  is  $\sim 10$  times slower than that of  $\text{Na}(\text{H}_2\text{O})_2$ , similar to the ratio observed by Schulz and coworkers for the decay times of  $\text{NaD}_2\text{O}$  and  $\text{Na}(\text{D}_2\text{O})_2$ . The ion signal is the sum of two contributions, which correlate to the  $p_1$  and  $p_2$  electron signal, respectively. For the experimental ion decay in Fig. 4c, we thus keep the relaxation times fixed at the above values and only refine the abundances of the two contributions. Fig. 4c shows that this leads to a consistent fit. The corresponding relaxation times  $\tau_1$  and  $\tau_2$  at a pump wavelength of 780 nm are identical to the values at 740 nm, which might not be surprising as the two pump energies differ by only 0.09 eV. The decay mechanism of the p-states is currently unclear. For larger  $\text{Na}(\text{H}_2\text{O})_n$  cluster, it was proposed that the energy transfer is explained by internal conversion of the electronic excitation into vibrations of the ground state, with the stretching modes of water playing an important role in the energy transfer process [10]. To gain deeper insight into the decay mechanism of  $\text{NaH}_2\text{O}$  and in particular the potential role of the stretching mode, comparative experiments with other NaX clusters are planned.

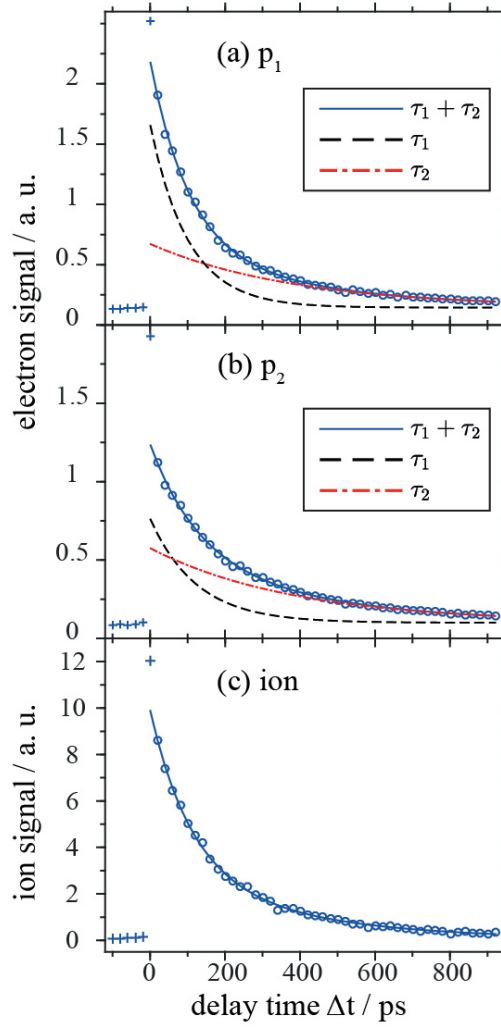


**Figure 4:** a) and b) Blue circles: Experimentally observed time-dependent decay of the electron signal for the photoelectron band  $p_1$  and  $p_2$  of NaH<sub>2</sub>O, respectively. Full blue line: Fit. Dashed black line: Fast decay  $\tau_1$ . Dashed-dotted red line: Slow decay  $\tau_2$ . c) Blue circles: Experimentally observed time-dependent decay of the NaH<sub>2</sub>O ion signal. Full blue line: Fit.

Fig. 5 shows a typical photoelectron image for delay times  $\Delta t > 20$  ps recorded at a pump wavelength of 740 nm. The inner and the middle ring correspond to the bands  $p_1$  and  $p_2$  of NaH<sub>2</sub>O, respectively. From Eq. (1), we have determined the anisotropy parameters as a function of delay time for  $\Delta t > 4$  ps for the two NaH<sub>2</sub>O bands. Within our uncertainty, we find identical anisotropy parameters of  $\beta_2 = 1.01 \pm 0.20$  and  $\beta_4 = 0.04 \pm 0.20$  for both bands independent of  $\Delta t$ . The same anisotropy parameters are also found for the deuterated species.

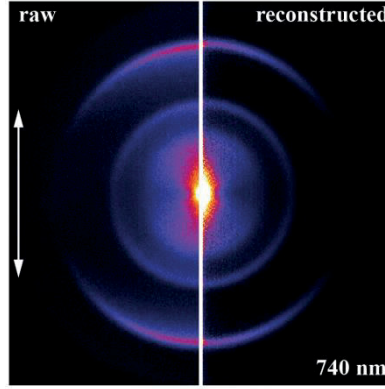


**Figure 5:** Typical photoelectron image for delay times  $\Delta t > 20$  ps recorded at a pump wavelength of 740 nm. Right: Raw image before reconstruction. Left: Reconstructed images. The arrow indicates the polarization direction of the pump and probe. The inner and the middle ring correspond to the bands  $p_1$  and  $p_2$  of  $\text{NaH}_2\text{O}$ , respectively, while the outer ring corresponds to the band  $p_4$  of  $\text{Na}^+$  (Fig. 2).

The identical lifetimes and anisotropy parameters of  $p_1$  and  $p_2$  and the insensitivity of the photoelectron anisotropy to isotopic substitution hint at a similar overall electronic character; i. e. singly excited  $3s(\text{Na}) \rightarrow 3p(\text{Na})$ . The values of the anisotropy parameters are in agreement with slightly disturbed p-states of a weakly-bound Na-complex. The corresponding values in the bare Na atom ( $^2P_{1/2}$ ) are  $\beta_2 = 1.77 \pm 0.10$  and  $\beta_4 = 0$  [50].

### 3.3 Energetics of $\text{NaH}_2\text{O}$ excitation

The experiments shown in Fig. 2 reveal two distinct photoelectron bands  $p_1$  and  $p_2$  at 1.68 eV pump energy (740 nm), but just one band  $p_1$  at 1.59 eV pump energy (780 nm). How can these two bands and the pump energy-dependence be explained? The local symmetry of the Na is broken by the  $\text{H}_2\text{O}$  molecule, essentially through the very weak  $\text{Na}\cdots\text{O}$  “bond”. In this local symmetry, the p-orbitals split into  $\sigma$  and  $\pi$  states.  $\sigma$  correlates with  $A_1$  in  $C_{2v}$  and  $\pi$  with  $B_1$  and  $B_2$ . This qualitative two-state picture also reflects in the geometry-dependence of the p-state energies (Fig. 1). The energy of the  $A_1$  ( $\sigma$ ) state shows a steep dependence on both the Na-O distance and the out-of-plane angle  $\delta$ , while the corresponding potential curves in the B-states ( $\pi$ ) are much flatter and similar to each other. Of course, the two state picture is only a coarse classification with details modified by multiple crossings and corresponding vibronic interactions. Fig. 1a shows the  $\delta$ -dependence at the Na-O ground state equilibrium distance  $r_{\text{Na-O, eq}}(X)$ . However, the p-states and the ion have Na-O equilibrium distances that are  $\sim 15$  pm shorter than in the ground state (Fig. 1b). In Fig. 6, we provide the equivalent to Fig. 1a,

at a Na-O distance that approximately corresponds to the p-state and ion equilibrium structure. The qualitative two-state picture is still retained. The p-states can be classified into one state that strongly depends on the geometry ( $A_1$ ) and two very similar states with a weak geometry-dependence ( $B_1$  and  $B_2$ ). Overall, the  $A_1$  state lies higher in energy and is preferentially localized around the  $C_{2v}$  geometry; in that it resembles more the ionic state, which shows the  $C_{2v}$  equilibrium structure of a semi-rigid molecule with a Na-O distance similar to the  $A_1$  p-state (Fig. 1b). The B-states (Fig. 6), in particular  $B_1$ , have a clear preference for pyramidal structures, with a potential minimum of  $B_1$  around  $\delta \sim 50^\circ$ . Note that the geometry and the vibrational frequencies of the  $H_2O$  unit remain virtually the same throughout.

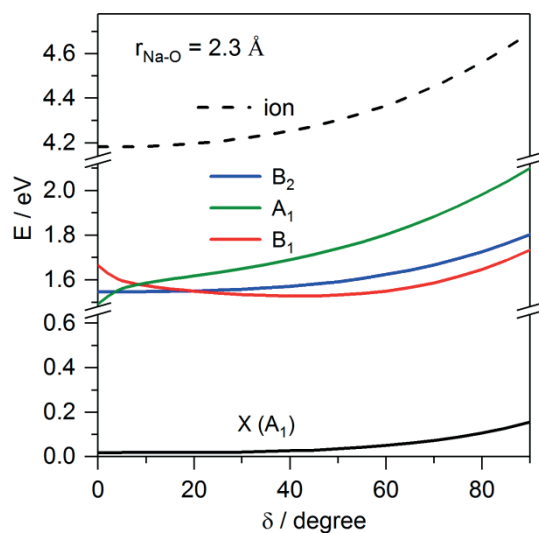


**Figure 6:** The same as in Fig. 1a, but for a Na-O distance of  $r_{\text{Na-O}} = 2.3 \text{ \AA}$  instead of the  $r_{\text{Na-O, eq}}(X)$  ground state equilibrium distance.

This situation has qualitative consequences for the Franck-Condon factors of the pump and probe steps. The energetically lowest excitation of the pump step is to the B-states, with a broad distribution over non-planar geometries. This leads to Franck-Condon factors that do not depend very sensitively on the exact pump energy. The probe step proceeds from this distribution to the more tightly-bound planar ion. As a result, this step has a preference for vibrationally excited ionic states, which means low eKE in the photoelectron spectrum. A (small) increase in the pump energy would add vibrational excitation in the B states – mainly in the intermolecular bending coordinates ( $b_1$  and  $b_2$  in  $C_{2v}$ ) - resulting in a more highly excited ion with virtually unchanged eKE. This is borne out by the behaviour of the low eKE peak  $p_1$ , which is observed at approximately the same eKE at the two different pump

wavelengths. From the experimental AIE we derive an average vibrational excitation of 0.14 eV at 780 nm and 0.23 eV at 740 nm. The extent of bending vibrational excitation is also reflected in the isotope dependence of the  $p_1$  peak. The change in zero point energies reduces the AIE by 0.007 eV, while deuteration lowers the intermolecular bending wavenumbers in the ion by about 0.01eV. The isotope shift of the intermolecular stretching vibration is negligible. Assuming the average excitation of one quantum of intermolecular bend at 780 nm and three quanta at 740 nm with the remainder in stretching excitation the corresponding peak  $p_1$  should shift by 0.017 eV and 0.037eV, respectively, to higher eKE values upon deuteration. Experimentally we indeed observe a small shift of about 0.01 eV at 780 nm and a more pronounced one of about 0.03 eV at 740 nm, both to higher eKE as expected.

The second band  $p_2$  is only observed at the higher pump energy (740 nm). This fits to the behaviour of the  $A_1$  state in Fig. 6, which can only be reached at higher pump energies than the B states. The lowest vibronic levels of the  $A_1$  state is localized around the  $C_{2v}$  geometry at a Na-O distance similar to the ion. It is plausible that excitation to this state has an appreciable Franck-Condon factor because the ground state vibrational function is broadly delocalized. Therefore, the Franck-Condon factor for the probe step starting from the lowest vibrational level of the  $A_1$  state preferentially leads to ionic states with low vibrational excitation and correspondingly higher eKEs. We observe band  $p_2$  at an eKE of 0.38 eV , which almost exactly matches the difference between the total photon energy of 4.78 eV and the AIE of  $\text{NaH}_2\text{O}$  of 4.38 eV. This means that  $p_2$  is on average associated with ions in their vibrational ground state. In agreement with this assignment the position of  $p_2$  hardly shifts upon deuteration. We determine an insignificant shift of  $\sim 0.003$  eV again to higher eKE, which compares well with the expected reduction of the AIE by 0.01 eV upon deuteration (experiment:  $0.009 \pm 0.002$  [35]).

#### 4. Conclusions

The  $\text{NaH}_2\text{O}$  complex describes the first step of the solvation of Na and how it modifies its electronic structure. The result is a remarkably complex structure of electronic levels with multiple crossings. The present experiments allow us to draw a coarse picture of the overall energetics of the first excited p-states. It turns out that the p-states fall into two classes, an almost degenerate pair with fairly shallow intermolecular potential curves and a third state that is closer to a semi-rigid behaviour and in that resembles the ionic state. The complexity

of vibronic interactions will make it difficult to unravel the finer details. Here, the experiment needs the support of advanced theory. The intriguing aspect of this system is that with state-of-the-art theoretical approaches it should be conceivable to describe the complete system in full dimensionality.

**Acknowledgment:** We thank Dr. David Luckhaus for help with the calculations and David Stapfer and Markus Steger for technical support. Financial support was provided by the ETH Zürich (projects ETH-01 15-2 and ETH-FAST/Signorell-2).

## REFERENCES

- [1] C.P. Schulz, R. Haugstätter, H.U. Tittes, I.V. Hertel, *Phys. Rev. Lett.* 57 (1986) 1703.
- [2] R.N. Barnett, U. Landman, *Phys. Rev. Lett.* 70 (1993) 1775.
- [3] C. Bobbert, S. Schütte, C. Steinbach, U. Buck, *Eur. Phys. J. D* 19 (2002) 183.
- [4] C. Steinbach, U. Buck, *J. Phys. Chem. A* 110 (2006) 3128.
- [5] E. Zurek, P.P. Edwards, R. Hoffmann, *Angew. Chem. Int. Ed.* 48 (2009) 8198.
- [6] L. Cwiklik, U. Buck, W. Kulig, P. Kubisiak, P. Jungwirth, *J. Chem. Phys.* 128 (2008) 154306.
- [7] C.P. Schulz, C. Bobbert, T. Shimosato, K. Daigoku, N. Miura, K. Hashimoto, *J. Chem. Phys.* 119 (2003) 11620.
- [8] S. Kondo, K. Hashimoto, H. Tachikawa, *Chem. Phys. Lett.* 431 (2006) 45.
- [9] K. Hashimoto, K. Daigoku, *Chem. Phys. Lett.* 469 (2009) 62.
- [10] H.T. Liu, J.P. Müller, N. Zhavoronkov, C.P. Schulz, I. Hertel, *J. Phys. Chem. A* 114 (2010) 1508.
- [11] J.P. Müller, N. Zhavoronkov, I.V. Hertel, C.P. Schulz, *J. Phys. Chem. A* 118 (2014) 8517.
- [12] A.H.C. West, B.L. Yoder, D. Luckhaus, R. Signorell, *J. Phys. Chem. A* 119 (2015) 12376.
- [13] A.H.C. West, B.L. Yoder, D. Luckhaus, C.-M. Saak, M. Doppelbauer, R. Signorell, *J. Phys. Chem. Lett.* 6 (2015) 1487.
- [14] S. Hartweg, A.H.C. West, B.L. Yoder, R. Signorell, *Angew. Chem. Int. Ed.* 55 (2016) 12347.
- [15] A.O. Gunina, A.I. Krylov, *J. Phys. Chem. A* 120 (2016) 9841.
- [16] H. Haberland, C. Ludewigt, H.G. Schindler, D.R. Worsnop, *Surface Science* 156 (1985) 157.
- [17] J.V. Coe, G.H. Lee, J.G. Eaton, S.T. Arnold, H.W. Sarkas, K.H. Bowen, C. Ludewigt, H. Haberland, D.R. Worsnop, *J. Chem. Phys.* 92 (1990) 3980.
- [18] J.R.R. Verlet, A.E. Bragg, A. Kammrath, O. Cheshnovsky, D.M. Neumark, *Science* 307 (2005) 93.
- [19] A.E. Bragg, J.R.R. Verlet, A. Kammrath, O. Cheshnovsky, D.M. Neumark, *J. Am. Chem. Soc.* 127 (2005) 15283.
- [20] L. Ma, K. Majer, F. Chiro, B. von Issendorff, *J. Chem. Phys.* 131 (2009) 144303.
- [21] R.M. Young, D.M. Neumark, *Chem. Rev.* 112 (2012) 5553.
- [22] J.M. Herbert, M.P. Coons, *Annu. Rev. Phys. Chem.* 68 (2017).
- [23] K.R. Siefert, Y. Liu, E. Lugovoy, O. Link, M. Faubel, U. Buck, B. Winter, B. Abel, *Nature Chem.* 2 (2010) 274.
- [24] Y. Yamamoto, S. Karashima, S. Adachi, T. Suzuki, *J. Phys. Chem. A* 120 (2016) 1153.
- [25] B.C. Garrett, D.A. Dixon, D.M. Camaioni, D.M. Chipman, M.A. Johnson, C.D. Jonah, G.A. Kimmel, J.H. Miller, T.N. Rescigno, P.J. Rossky, S.S. Xantheas, S.D. Colson, A.H. Laufer, D. Ray, P.F. Barbara, D.M. Bartels, K.H. Becker, H. Bowen, S.E. Bradforth, I. Carmichael, J.V. Coe, L.R. Corrales, J.P. Cowin, M. Dupuis, K.B. Eisenthal, J.A. Franz, M.S. Gutowski, K.D. Jordan, B.D. Kay, J.A. LaVerne, S.V. Lymar, T.E. Madey, C.W. McCurdy, D. Meisel, S. Mukamel, A.R. Nilsson, T.M. Orlando, N.G. Petrik, S.M. Pimblott, J.R. Rustad, G.K. Schenter, S.J. Singer, A. Tokmakoff, L.S. Wang, C. Wittig, T.S. Zwier, *Chem. Rev.* 105 (2005) 355.
- [26] E. Alizadeh, T.M. Orlando, L. Sanche, *Annu. Rev. Phys. Chem.* 66 (2015) 379.
- [27] K. Yokoyama, C. Silva, D.H. Son, P.K. Walhout, P.F. Barbara, *J. Phys. Chem. A* 102 (1998) 6957.
- [28] M.H. Elkins, H.L. Williams, A.T. Shreve, D.M. Neumark, *Science* 342 (2013) 1496.



- [29] S. Karashima, Y. Yamamoto, T. Suzuki, *Phys. Rev. Lett.* 116 (2016) 137601.
- [30] D.R. Yarkony, *Chem. Rev.* 112 (2012) 481.
- [31] P.W. Forysinski, P. Zielke, D. Luckhaus, R. Signorell, *Phys. Chem. Chem. Phys.* 12 (2010) 3121.
- [32] D. Luckhaus, P.W. Forysinski, P. Zielke, R. Signorell, *Mol. Phys.* 108 (2010) 2325.
- [33] M. Head-Gordon, R.J. Rico, M. Oumi, T.J. Lee, *Chem. Phys. Lett.* 219 (1994) 21.
- [34] C.W. Bauschlicher, S.R. Langhoff, H. Partridge, J.E. Rice, A. Komornicki, *J. Chem. Phys.* 95 (1991) 5142.
- [35] D.A. Rodham, G.A. Blake, *Chem. Phys. Lett.* 264 (1997) 522.
- [36] J.E. Sansonetti, *J. Phys. Chem. Ref. Data* 37 (2008) 1659.
- [37] A.H.C. West, B.L. Yoder, R. Signorell, *J. Phys. Chem. A* 117 (2013) 13326.
- [38] B.L. Yoder, A.H.C. West, B. Schläppi, E. Chasovskikh, R. Signorell, *J. Chem. Phys.* 138 (2013) 044202.
- [39] B.L. Yoder, J.H. Litman, P.W. Forysinski, J.L. Corbett, R. Signorell, *J. Phys. Chem. Lett.* 2 (2011) 2623.
- [40] B. Schläppi, J.J. Ferreiro, J.H. Litman, R. Signorell, *Int. J. Mass Spectrom.* 372 (2014) 13.
- [41] R. Signorell, M. Goldmann, B.L. Yoder, A. Bodi, E. Chasovskikh, L. Lang, D. Luckhaus, *Chem. Phys. Lett.* 658 (2016) 1.
- [42] B. Dick, *Phys. Chem. Chem. Phys.* 16 (2014) 570.
- [43] K.L. Reid, *Annu. Rev. Phys. Chem.* 54 (2003) 397.
- [44] M.M. Kappes, M. Schär, U. Röthlisberger, C. Yerezian, E. Schumacher, *Chem. Phys. Lett.* 143 (1988) 251.
- [45] R.T. Carter, J.R. Huber, *Chem. Soc. Rev.* 29 (2000) 305.
- [46] R.M. Bowman, M. Dantus, A.H. Zewail, *Chem. Phys. Lett.* 161 (1989) 297.
- [47] J.R.R. Verlet, V.G. Stavros, R.S. Minns, H.H. Fielding, *J. Phys. B: At., Mol. Opt. Phys.* 36 (2003) 3683.
- [48] M. Lucchini, A. Ludwig, T. Zimmermann, L. Kasmi, J. Herrmann, A. Scrinzi, A.S. Landsman, L. Gallmann, U. Keller, *Phys. Rev. A* 91 (2015) 063406.
- [49] D.C. Morton, *Astrophys. J. Suppl. Ser.* 149 (2003) 205.
- [50] J.A. Duncanson, M.P. Strand, A. Lindgård, R.S. Berry, *Phys. Rev. Lett.* 37 (1976) 987.